Microstrip cross-coupled trisection bandpass filters with asymmetric frequency characteristics

J.-S. Hong
M.J. Lancaster

Abstract: A pair of microstrip trisection bandpass filters, consisting of cross-coupled open-loop resonators and exhibiting asymmetric frequency characteristics, are introduced. The utilisation of the microstrip open-loop resonators not only makes the filters compact, but also allows either positive or negative cross coupling to be realised. This results in an attenuation pole of finite frequency on either the high side or the low side of the pass band, so that the frequency response is asymmetric. Two filter designs of this type are described. Theoretical and experimental results are presented

1 Introduction

High selectivity and low pass-band insertion loss of RF/microwave bandpass filters are required for many applications, including the rapidly expanding area of mobile communications systems. These requirements are imposed to conserve the valuable frequency spectrum and enhance the performance of the systems. For example, the highly selective channel filters are able to minimise the guard band between adjacent channels so as to use the frequency spectrum more efficiently. Although the low insertion loss filters can increase the sensitivity of communications systems, in general, a bandpass filter can achieve a higher selectivity by increasing the degree of poles, i.e. the number of resonators. However, because the quality factor of resonators is finite, the pass-band insertion loss of the filter is increased as the number of resonators increases. Therefore, there is always a trade-off between the selectivity and the pass-band insertion loss. On the other hand, for a specified filter selectivity, we could select a certain type of filter characteristics that not only meets the selectivity requirement, but also results in a minimum pass-band insertion loss for a given quality factor of the resonators. Furthermore, some applications of bandpass filters may require a higher selectivity on only one side of the pass band, but less or none on the other side. In such cases, using a filter with asymmetric frequency characteristics would be desirable [1–5]. This is because a symmetric frequency-response filter results in a larger number of resonators with a higher insertion loss in the pass band, a larger size and a higher cost.

IEE Proceedings online no. 19990146

DOI: 10.1049/ip-map:19990146

Paper received 3 June 1998

The authors are with the University of Birmingham, School of Electronic and Electrical Engineering, Edgbaston, Birmingham B15 2TT, UK

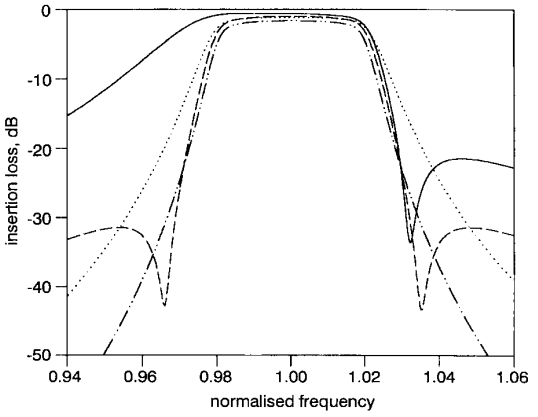

Fig. 1 *Transmission response of bandpass filter to meet simple specification: rejection larger than 20dB for normalised frequency ≥ 1.03 and return loss ≤ –20dB over fractional bandwidth FBW = 0.035, Q_u = 500*
····· 4-pole Chebyshev ——— 3-pole asymmetric – – – 4-pole elliptic –·–· 5-pole Chebyshev

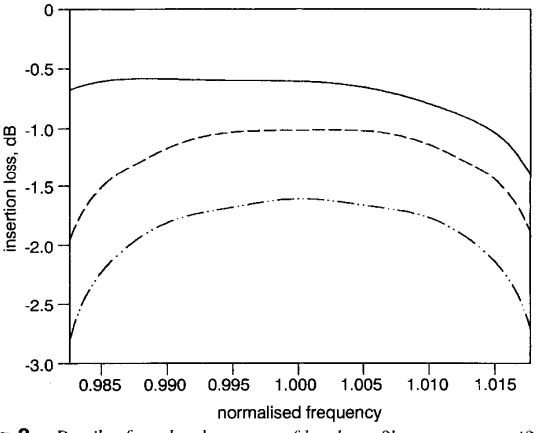

Fig. 2 *Details of passband response of bandpass filter to meet specification given in Fig. 1*
——— 3-pole asymmetric – – – 4-pole elliptic –·–· 5-pole Chebyshev

For our demonstration, Figs. 1 and 2 show a comparison of different types of bandpass filter responses to meet the simple specifications of a rejection larger than 20dB for the normalised frequencies ≥ 1.03, and a return loss ≤ –20dB over a fractional bandwidth *FBW* = 0.035. As can be seen in Fig. 1, the four-pole Chebyshev filter does not meet the rejection requirement, but the five-pole Chebyshev filter does. The four-pole elliptic or quasi-elliptic flinction response filter with a pair of attenuation poles or transmission zeros at finite frequencies meets the specifications. However, the most

notable thing is that the three-pole filter with an asymmetric frequency response not only meets the specifications, as well, but also results in the smallest pass-band insertion loss as compared with the other filters: the latter is clearly illustrated in Fig. 2.

The above example illustratively shows the attractive features of bandpass filters having asymmetric frequency characteristics, which may be interesting for duplexer applications. Such asymmetric frequency characteristics can normally be realised by cross-coupled filter configurations [1–5]. There have been different types of microstrip bandpass filters [5–15]. However, owing to difficulties in arranging and controlling cross-couplings in microstrip circuit topologies, only very few microstrip filters have been designed to have asymmetric frequency characteristics [5]. Therefore, it is our aim to introduce a pair of microstrip cross-coupled trisection bandpass filters that are developed to exhibit the asymmetric frequency characteristics. Our microstrip trisection bandpass filters consist of cross-coupled open-loop resonators. We show that the utilisation of the microstrip open-loop resonators not only makes the filters compact, but also allows either positive or negative cross-coupling to be realised. This results in an attenuation pole of finite frequency on either the high side or the low side of the pass band, so that the frequency response is asymmetric. The two filter designs, one with an attenuation pole on the high side of the pass band and the other with an attenuation pole on the low side of the pass band, are presented with both the theoretical and experimental results.

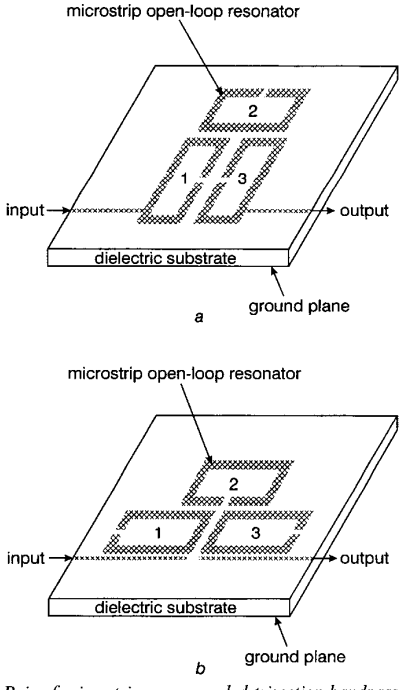

Fig.3 *Pair of microstrip cross-coupled trisection bandpass filters exhibiting asymmetric frequency response*
a Filter with higher selectivity on high side of passband
b Filter with higher selectivity on low side of passband

2 Microstrip cross-coupled trisection filters

The configurations of the proposed microstrip cross-coupled trisection bandpass filters are shown in Fig. 3. Each of the filters is composed of three open-loop resonators on one side of the dielectric substrate with a ground plane on the other side. The input and output are coupled through tapped lines in Fig. 3*a* or coupled lines in Fig. 3*b* to resonators 1 and 3, respectively. It is obvious that the cross coupling between resonators 1 and 3 exists because of their proximity.

We show later that, as a result of the cross coupling, the filter configuration of Fig. 3*a* has an attenuation pole of finite frequency on the high side of the pass band, whereas the filter configuration of Fig. 3*b* produces an attenuation pole of finite frequency on the low side of the pass band. For the narrowband case, both of the filters may be represented by an equivalent circuit of Fig. 4. The couplings between adjacent resonators are indicated by the coupling coefficients M_{12} and M_{23}, and the cross coupling is denoted by M_{13}. Q_{ei} and Q_{eo} are the external quality factors denoting the input and output couplings, respectively. Note that because it is not necessary for the resonators to be synchronously tuned for this type of filter, $1/\sqrt{L_nC_n} = \omega_{0n}$ is the resonant angular frequency of resonator n for $n = 1$, 2 and 3. Although we want the frequency response of trisection filters to be asymmetric, the physical configurations of the filters can be kept symmetric. Therefore, for simplicity, we can let $M_{12} = M_{23}$, $Q_{ei} = Q_{eo}$ and $\omega_{01} = \omega_{03}$.

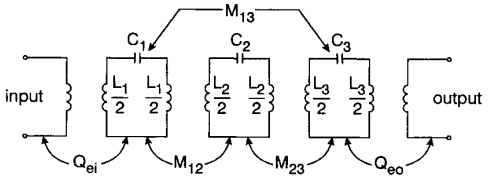

Fig.4 *Equivalent circuit of 3-pole cross-coupled bandpass filter*

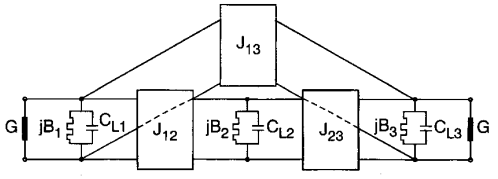

Fig.5 *Associated low-pass prototype filter*

One approach to design this type of filter is to find all the circuit parameters in Fig. 4, i.e. the coupling coefficients, the external quality factors and the resonant frequencies for microstrip implementation. This may be done in the light of a lowpass prototype filter shown in Fig. 5. Each of the rectangular boxes represents a frequency invariant immittance inverter, with J the characteristic admittance of the inverter. In our case $J_{12} = J_{23} = 1$ for the inverters along the main path of the filter. The bypass inverter with a characteristic admittance J_{13} accounts for the cross coupling. C_{Ln} and B_n ($n = 1$, 2, 3) denote the capacitance and the frequency invariant susceptance of the lowpass prototype filter, respectively. For the symmetry $C_{L1} = C_{L3}$ and $B_1 = B_3$; $G = 1$ is the normalised terminal. The unknown lowpass element values may be determined by a synthesis method [16] or through an optimisation process. Once they are determined, the circuit parameters in Fig. 4 can be found by

$$\omega_{0n} = \omega_0\sqrt{1 - \frac{B_n}{C_{Ln}/FBW + B_n/2}} \quad \text{for } n = 1, 2 \text{ and } 3 \tag{1}$$

$$Q_{ei} = Q_{eo} = \frac{\omega_{01}}{\omega_0}\left(\frac{C_{L1}}{FBW} + \frac{B_1}{2}\right) \quad (2)$$

$$M_{12} = M_{23} = \frac{\omega_0}{\sqrt{\omega_{01}\omega_{02}}} \times \frac{FBW}{\sqrt{(C_{L1} + FBW \cdot B_1/2)(C_{L2} + FBW \cdot B_2/2)}} \quad (3)$$

$$M_{13} = \frac{\omega_0}{\sqrt{\omega_{01}\omega_{03}}} \times \frac{FBW \cdot J_{13}}{\sqrt{(C_{L1} + FBW \cdot B_1/2)(C_{L3} + FBW \cdot B_3/2)}} \quad (4)$$

Here ω_0 is the midband frequency and FBW is the fractional bandwidth of the bandpass filters. In eqn. 1 we can clearly see that the effect of frequency invariant susceptance is the offset of the resonant frequency of a shunt resonator from the midband frequency of the bandpass filter. Therefore, as we mentioned before, the bandpass filter of this type is in general asynchronously tuned. This is why the formulations of the external quality factor and coupling coefficients differ from those for a synchronously tuned filter [15]. Nevertheless, note that if the frequency-invariant susceptances vanish, the formulations are degenerated to those for the synchronously tuned filter. The derivation of eqns. 1 to 4 is given in the Appendix.

It can be shown that if the cross coupling is positive, i.e. $M_{13} > 0$ or $J_{13} > 0$, the attenuation pole of finite frequency is on the high side of the pass band, whereas if the cross coupling is negative, i.e. $M_{13} < 0$ or $J_{13} < 0$, the attenuation pole of finite frequency is on the low side of the pass band. We demonstrate that the filter configuration of Fig. 3*a* has an attenuation pole of finite frequency above the pass band, whereas the filter configuration of Fig. 3*b* has an attenuation pole of finite frequency below the pass band owing to the cross coupling between resonators 1 and 3. Hence, we should refer to the cross coupling of resonators 1 and 3 in Fig. 3*a* as the positive coupling, and to the cross coupling of resonators 1 and 3 in Fig. 3*b* as the negative coupling. Note that the meaning of positive or negative coupling is rather relative. This means that if we refer to one particular coupling as the positive coupling, then the negative coupling would imply that its phase response is opposite to that of the positive coupling. This may be demonstrated using full-wave simulation of frequency responses of the coupled microstrip open-loop resonators, as shown in Figs. 6 and 7. Note that the electric coupling of Fig. 6 is referred to the coupling between resonators 1 and 3 in Fig. 3*a* because the electric fringe field is dominant for the coupling, and the magnetic coupling of Fig. 7 is referred to the coupling between resonators 1 and 3 in Fig. 3*b* on the grounds that the magnetic fringe field is dominant. As can be seen, the phase responses of the two types of couplings are indeed opposite.

3 Filter design: example one

The first filter design example is the type shown in Fig. 3*a*. For our demonstration the filter is designed to meet the following specifications:

midband or centre frequency = 905MHz
bandwidth of pass band = 40MHz
return loss in the pass band < –20dB
rejection >20dB for frequencies ≥ 950MHz

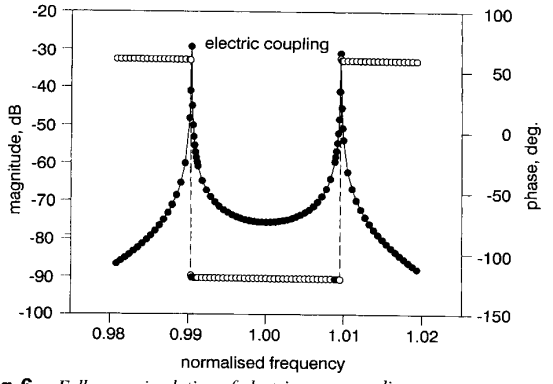

Fig. 6 *Full-wave simulation of electric cross coupling*
—•— magnitude —○— phase

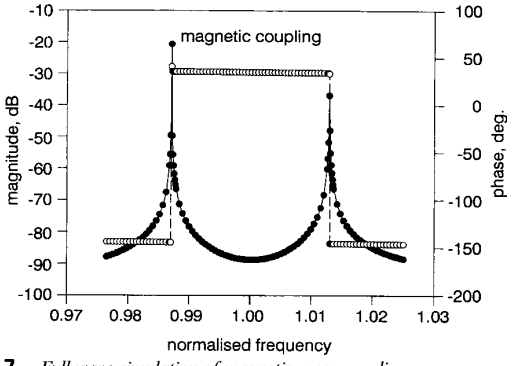

Fig. 7 *Full-wave simulation of magnetic cross coupling*
—•— magnitude —○— phase

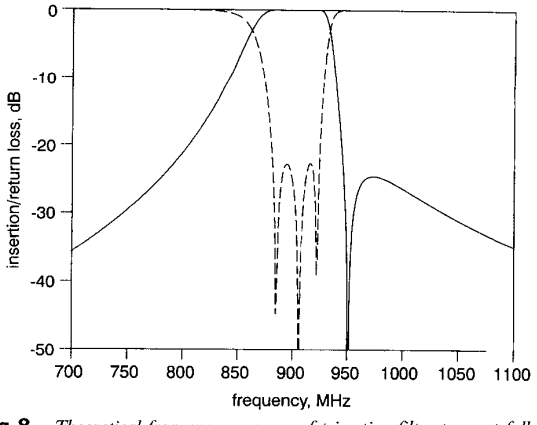

Fig. 8 *Theoretical frequency response of trisection filter to meet following specifications: return loss < –20dB over passband of 885MHz to 925MHz, (thus f_0 = 905MHz, FBW = 0.0442), out of band rejection > 20dB for f ≥ 950MHz*
——— insertion loss - - - return loss

Thus, the fractional bandwidth is 4.42%. The element values of the lowpass prototype filter are found to be $C_{L1} = C_{L3} = 0.695$, $B_1 = B_3 = 0.185$, $C_{L2} = 1.245$, $B_2 = -0.615$ and $J_{13} = 0.457$. Shown in Fig. 8 is the theoretical frequency response of the filter. To realise the filter in the microstrip open-loop resonator configuration, the resonant frequencies, the external quality factors

and the coupling coefficients are calculated using eqns. 1–4. It turns out that

$$\omega_{01} = \omega_{03} = 899.471 \text{ MHz}$$
$$\omega_{02} = 914.713 \text{ MHz}$$
$$Q_{ei} = Q_{eo} = 15.7203$$
$$M_{12} = M_{23} = 0.04753$$
$$M_{13} = 0.02907 \quad (5)$$

We can see that the resonant frequency of resonators 1 and 3 is lower than the midband frequency, whereas the resonant frequency of resonator 2 is higher than the midband frequency. The frequency offsets amount to −0.61% and 1.07%, respectively. The physical dimensions of the microstrip trisection filter can be determined using an procedure similar to that described in [14, 15]. The filter is then fabricated on an RT/Duroid 6010 substrate, with a relative dielectric constant of 10.8 and a thickness of 1.27mm. Fig. 9 is a photograph of the fabricated filter. The size of the filter is about 0.19 λ_{g0} by 0.27 λ_{g0}, where λ_{g0} is the guided wavelength of a 50-ohm line on the substrate at the midband frequency. This size is evidently very compact. The filter is tested using an HP 8510 network analyser.

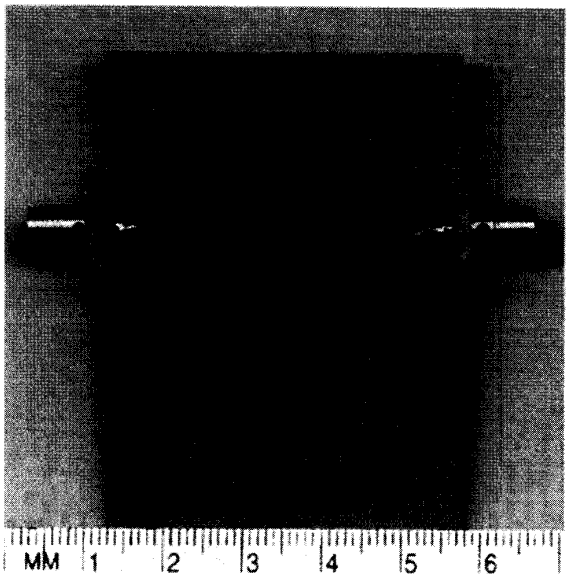

Fig. 9 *Photograph of fabricated microstrip trisection bandpass filter with attenuation pole of finite frequency on upper side of pass band*

Fig. 10 shows the measured results of the filter with slight tuning. The tuning is needed because of the tolerances of fabrication and substrate. As can be seen, an attenuation pole of finite frequency on the upper side of the pass band leads to a higher selectivity on this side of the pass band. The measured return loss in the pass band is below −20dB as desired by the design. The midband insertion loss is about −1.15dB, which is mainly owing to the conduction loss of the microstrip which is made out of copper. The measured wide-band response is given in Fig. 11. It seems that the effect of cross coupling produces attenuation poles on the low side of the harmonic responses. This results in a wider stopband between the fundamental and the first spurious response.

4 Filter design: example two

The second filter design example is the type shown in Fig. 3*b* for an attenuation pole on the low side of the pass band. The filter is designed to meet the following specifications:

midband or centre frequency = 910MHz

bandwidth of pass band = 40MHz

return loss in the pass band < −20dB

rejection > 35dB for frequencies ≤ 843MHz

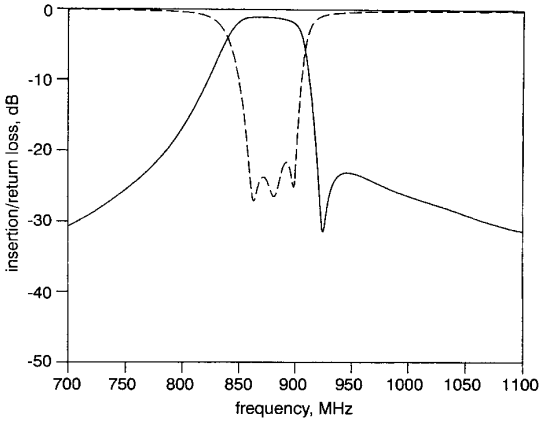

Fig. 10 *Measured filter performance for first filter design example*
——— *insertion loss* – – – *return loss*

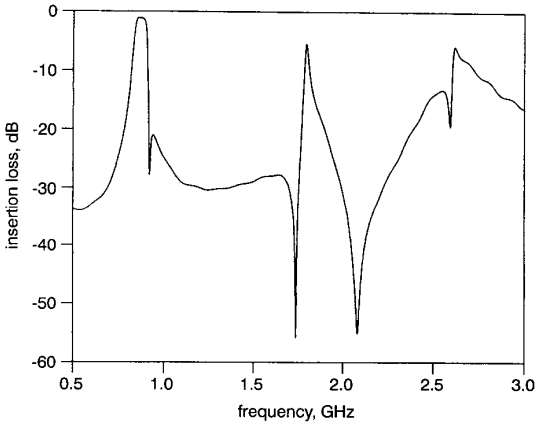

Fig. 11 *Measured wide-band frequency response of first filter design example*

The element values of the lowpass prototype filter for this design example are $C_{L1} = C_{L3} = 0.645$, $B_1 = B_3 = -0.205$, $C_{L2} = 0.942$, $B_2 = 0.191$ and $J_{13} = -0.281$. Note that, in this case, the frequency invariant susceptances and the characteristic admittance of the cross-coupling inverter have the opposite signs as referred to those of the above filter design. Shown in Fig. 12 is the theoretical frequency response of the filter with an attenuation pole of finite frequency below the pass band. The resonant frequencies, the external quality factors and the coupling coefficients of the microstrip open-loop resonator trisection filter in Fig. 3*b* are found to be

$$\omega_{01} = \omega_{03} = 916.159 \text{ MHz}$$
$$\omega_{02} = 905.734 \text{ MHz}$$
$$Q_{ei} = Q_{eo} = 14.6698$$

$$M_{12} = M_{23} = 0.05641$$
$$M_{13} = -0.01915 \tag{6}$$

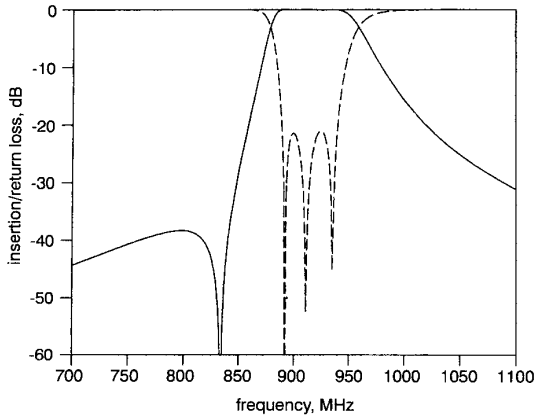

Fig. 12 *Theoretical frequency response of trisection filter to meet following specifications: return loss < –20dB over passband of 890MHz to 930MHz, (thus f_0 = 910MHz, FBW = 0.044), out of band rejection > 35dB for f ≤ 843MHz*
——— insertion loss – – – return loss

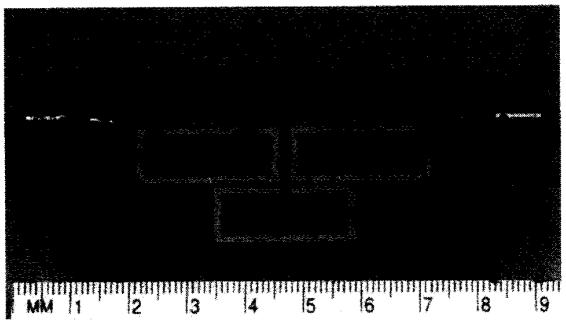

Fig. 13 *Photograph of microstrip trisection bandpass filter with attenuation pole of finite frequency on low side of pass band*

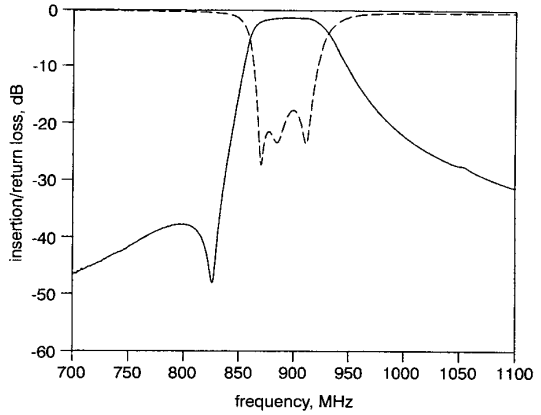

Fig. 14 *Measured filter performance of second design example*
——— *insertion loss – – – return loss*

In contrast to the design example in Section 3, the resonant frequency of resonators 1 and 3 is higher than the midband frequency, whereas the resonant frequency of resonator 2 is lower than the midband frequency. The frequency offsets are 0.68% and –0.47%, respectively. Moreover, the cross-coupling coefficient is negative. Similarly, the filter is fabricated on an RT/Duroid 6010 substrate with a relative dielectric constant of 10.8 and a thickness of 1.27mm. Fig. 13 shows a photograph of the fabricated filter. The size of the filter amounts to 0.41 λ_{g0} by 0.17 λ_{g0}. The measured results of the filter are plotted in Fig. 14. The attenuation pole of finite frequency does occur on the low side of the pass band so that the selectivity on this side is higher than that on the upper side. The return loss in the pass band is below –17dB and the midband insertion loss is about –1.28dB. Again the insertion loss is mainly attributed to the conductor loss. The measured wide-band response is given in Fig. 15. The spurious response of this filter is not quite the same as that of the filter presented above.

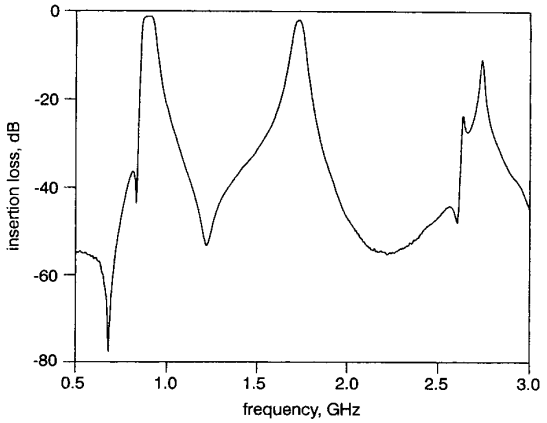

Fig. 15 *Measured filter wide-band frequency response of second filter design example*

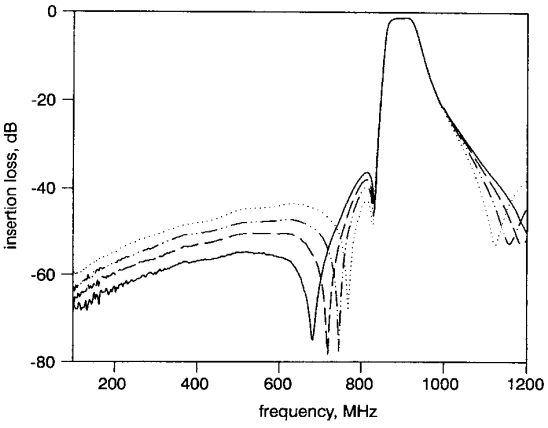

Fig. 16 *Experimental results on extra transmission zero of second microstrip trisection filter design example, where cases 1 to 4 indicate the increase of direct coupling between the two feed lines*
——— case 1 – – – case 2 –·–·– 5-pole case 3 ····· case 4

The most interesting observation is that there exists an extra attenuation pole below the frequency location of the designed attenuation pole. It would seem that this extra attenuation pole results from an extra cross coupling between the two input and output feed lines. Using a dielectric tuning element to alter the coupling between the two feed lines, we find that the altering of the coupling has much more effect on the extra attenuation pole. As the coupling is increased, the frequency location of the extra attenuation pole is moved inwards towards that of the designed one, causing the side-lobe of the designed attenuation pole to fall down at the cost of increasing the side-lobe of the extra attenuation

pole itself. However, the frequency location of the designed attenuation pole is hardly changed. This can clearly be seen from the experimental results as shown in Fig. 16, where cases 1 to 4 indicate the increased coupling between the open ends of two feed lines. You might also notice that on the high side of the pass band there is another attenuation pole which seems dependent on the cross coupling between the input and output as well.

5 Conclusions

Asymmetric frequency characteristics of RF/microwave bandpass filters can have advantages in certain applications. We have introduced a pair of microstrip trisection bandpass filters, which consist of cross-coupled open-loop resonators and exhibit asymmetric frequency characteristics. We have shown that the utilisation of the microstrip open-loop resonators not only makes the filters compact, but also allows either positive or negative cross coupling to be realised. The latter feature can result in an attenuation pole of finite frequency on either the high side or the low side of the pass band so that the frequency response is asymmetric. Two filter designs of this type, together with theoretical and experimental results, have been described. It can be seen that the microstrip cross-coupled trisection bandpass filters hold promise for mobile communications and other applications. The use of high-temperature superconductors can considerably improve their performance [17]. It can also be expected that the asymmetric frequency response microstrip filters with more than three resonators can be developed based on the proposed trisection filter configurations.

6 Acknowledgments

Dr. Lancaster was supported by the Nuffield Foundation.

7 References

1 KURZROK, R.M.: 'General three-resonator filters in waveguide', *IEEE Trans., Microwave Theory Tech.*, 1966, **MTT-14**, pp. 46–47

2 FRANTI, L.F., and PAGANUZZI, G.M.: 'Odd-degree pseudoelliptical phase-equalized filter with asymmetric bandpass behaviour'. Proceedings of European *Microwave* conference, Amsterdam, September 1981, pp. 111–116

3 CAMERON, R.J.: 'Dual-mode realisation for asymmetric filter characteristics', *ESA J.*, 1982, **6**, pp. 339–356

4 HERSHTIG, R., LEVY, R., and ZAKI, K.: 'Synthesis and design of cascaded trisection (CT) dielectric resonator filters'. Proceedings of European *Microwave* conference, Jerusalem, September 1997, pp. 784–791

5 MANSOUR, R.R., RAMMO, F., and DOKAS, V.: 'Design of hybrid-coupled multiplexers and diplexers using asymmetrical superconducting filters', *IEEE MTT-S Int. Microw. Symp. Dig.*, 1993, pp. 1281–1284

6 COHN, S.B.: 'Parallel-coupled transmission-line-resonator filters', *IEEE Trans.*, 1958, **MTT-6**, pp. 223–231

7 CRISTAL, E.G., and FRANKEL, S.: 'Hairpin-line and hybrid hairpin-line/half-wave parallel-coupled-line filters', *IEEE Trans.*, 1972, **MTT-20**, pp. 719–728

8 SAGAWA, M., TAKAHASHI, K., and MAKIMOTO, M.: 'Miniaturized hairpin resonator filters and their application to receiver front-end MIC's', *IEEE Trans.*, 1989, **MTT-37**, pp. 1991–1997

9 ZHANG, D.W., LIANG, G.-C., SHIH, C.F., WITHERS, R.S., JOHANSSON, M.E., and CRUZ, A.D.: 'Compact forward-coupled superconducting microstrip filters for cellular communication', *IEEE Trans.*, 1995, **AS-5**, (2), pp. 2656–2659

10 MATTAEI, G.L., FENZI, N.O., FORSE, R., and ROHLFING, S.: 'Narrow-band hairpin-comb filters for HTS and other applications', *IEEE MTT-S Int. Microw. Symp. Dig.*, 1996, pp. 457–460

11 WOLFF, I.: 'Microstrip bandpass filter using degenerate modes of a microstrip ring resonator', *Electron. Lett.*, 1972, **8**, pp. 302–303

12 CURTIS, J.A., and FIEDZIUSZKO, S.J.: 'Miniature dual mode microstrip filters', *IEEE MTT-S Int. Microw. Symp. Dig.*, 1991, pp. 443–446

13 HONG, J.-S., and LANCASTER, M.J.: 'Recent advances in microstrip filters for communications and other applications'. IEE Colloquium on *Advances in passive microwave components*, London, UK, 22 May 1997, pp. 2/1–2/6

14 HONG, J.-S., and LANCASTER, M.J.: 'Couplings of microstrip square open-loop resonators for cross-coupled planar microwave filters', *IEEE Trans.*, 1996, **MTT-44**, (12), pp. 2099–2109

15 HONG, J.-S., and LANCASTER, M.J.: 'Theory and experiment of novel microstrip slow-wave open-loop resonator filters', *IEEE Trans.*, 1997, **MTT-45**, (12), pp. 2358–2365

16 CHAMBER, D., and RHODES, J.D.: 'Asymmetric synthesis'. Proceedings of European *Microwave* conference, Amsterdam, September 1981, pp. 105–110

17 LANCASTER, M.J.: 'Passive microwave device applications of high temperature superconductors' (Cambridge University Press, Cambridge, UK, 1997)

18 MATTHAEI, G.L., YONG, L., and JONES, E.M.T.: 'Microwave filters, impedance matching networks, and coupling structures' (McGraw Hill Book Co., New York, 1964), Chap. 8

8 Appendix

Let us transfer a nodal capacitance and its associated frequency invariant susceptance of the lowpass prototype filter of Fig. 5 into a shunt resonator of the bandpass filter of Fig. 4. Using the well known lowpass to bandpass frequency transformation, we have

$$\frac{1}{FBW}\left(\frac{j\omega}{\omega_0}+\frac{\omega_0}{j\omega}\right)C_{Ln}+jB_n = j\omega C_n+\frac{1}{j\omega L_n} \quad (7)$$

Derivation of eqn. 7 with respect to $j\omega$ yields

$$\frac{1}{FBW}\left(\frac{1}{\omega_0}-\frac{\omega_0}{(j\omega)^2}\right)C_{Ln} = C_n-\frac{1}{(j\omega)^2 L_n} \quad (8)$$

Letting $\omega = \omega_0$ in eqns. 7 and 8 gives

$$B_n = \omega_0 C_n - \frac{1}{\omega_0 L_n} \quad (9a)$$

$$\frac{1}{FBW}\left(\frac{2}{\omega_0}\right)C_{Ln} = C_n+\frac{1}{\omega_0^2 L_n} \quad (9b)$$

We can solve for C_n and L_n

$$C_n = \frac{1}{\omega_0}\left(\frac{C_{Ln}}{FBW}+\frac{B_n}{2}\right) \quad (10a)$$

$$L_n = \frac{1}{\omega_0}\left(\frac{C_{Ln}}{FBW}-\frac{B_n}{2}\right)^{-1} \quad (10b)$$

and thus

$$\omega_{0n} = \frac{1}{\sqrt{L_n C_n}} = \omega_0\sqrt{1-\frac{B_n}{C_{Ln}/FBW+B_n/2}} \quad (11)$$

This is identical to eqn. 1. In order to derive the expressions for the external quality factors and coupling coefficients, we define a susceptance slope parameter of each shunt resonator in Fig. 4 as [18]

$$b_n = \frac{\omega_{0n}}{2}\frac{d}{d\omega}\left(\omega C_n-\frac{1}{\omega L_n}\right)\omega=\omega_{0n} \quad (12)$$

Substituting eqn. 10*a* and *b* into eqn. 12 yields

$$b_n = \omega_{0n}C_n = \frac{\omega_{0n}}{\omega_0}\left(\frac{C_{Ln}}{FBW}+\frac{B_n}{2}\right) \quad (13)$$

By using the definitions similar to those described previously [18] for the external quality factor and the coupling coefficient, we have

$$Q_{ei} = Q_{eo} = \frac{b_1}{G} \tag{14}$$

$$M_{12} = M_{23} = \frac{J_{12}}{\sqrt{b_1 b_2}} \tag{15}$$

$$M_{13} = \frac{J_{13}}{\sqrt{b_1 b_3}} \tag{16}$$

Substituting eqn. 13 into eqns. 14, 15 and 16 leads directly to eqns. 2, 3 and 4 if we recall that $G = 1$ and $J_{12} = 1$ in our case.